Int J Adv Manuf Technol (2017) 90:2109–2119
DOI 10.1007/s00170-016-9443-1

ORIGINAL ARTICLE

Influence of die parameters on the deformation inhomogeneity of transitional region during local loading forming of Ti-alloy rib-web component

Pengfei Gao[1] · Xiaodi Li[1] · He Yang[1] · Xiaoguang Fan[1] · Zhenni Lei[1]

Received: 16 June 2016 / Accepted: 4 September 2016 / Published online: 10 October 2016

Abstract The deformation inhomogeneity of transitional region plays a great role in both the macro and micro forming qualities in the local loading forming. In this work, the dependence of deformation inhomogeneity of transitional region on the die parameters in the local loading forming of Ti-alloy rib-web component was studied based on finite element (FE) simulation. To evaluate the deformation inhomogeneity, an area-weighted strain inhomogeneity index was employed, which is calculated through the user subroutine of FE software (DEFORM-2D). It is found that there exist two kinds of strain concentration areas contributing to the deformation inhomogeneity of transitional region. One kind is the almost symmetric strain concentration area at the non-partitioned ribs, which is essentially related to the filling of rib. Another kind is the slant strain concentration area at the partitioned rib, which is caused by the multi-step loading during local loading forming. Besides, the effects of die parameters on the deformation inhomogeneity of transitional region were studied by the combination of orthogonal experiment design and FE simulation. The results suggest that the draft angle of the right rib is the most significant factor for both the deformation inhomogeneities of the partitioned rib region and whole transitional region. And, these two deformation inhomogeneities both decrease with the draft angle of the right rib decreasing. Furthermore, the relationship between die parameters and deformation inhomogeneity of transitional region is developed using the response surface methodology (RSM). Based on the RSM model, the die parameters were optimized to improve the deformation homogeneity of transitional region. The results will provide basis for the design of die parameters to improving the deformation and microstructure homogeneities in the isothermal local loading forming of Ti-alloy rib-web component.

Keywords Local loading forming · Rib-web component · Transitional region · Die parameters · Deformation inhomogeneity

✉ He Yang
yanghe@nwpu.edu.cn

[1] State Key Laboratory of Solidification Processing, School of Materials Science and Engineering, Northwestern Polytechnical University, P.O. Box542, Xi'an 710072, People's Republic of China

1 Introduction

The isothermal local loading forming technology proposed by Yang et al. [1–4] integrates the advantages of local loading forming and isothermal forming. It can control the material flow, reduce the forming load, enhance the formability of material, and enlarge the size of component. These advantages make it a highly attractive way to form the titanium alloy large-scale complex components with thin web and high rib (such as bulk head), which have gained increasing applications in aviation field due to their features of high performance, light weight, and high reliability [4–7]. These components often serve as the key load-bearing structures under severe working conditions, so high quality of macroscopically forming and fine microstructure are both required in the forming process.

During local loading forming, the load is applied to part of the billet in one loading step and the component is formed by changing loading region. The alternation of loading region results in the loading region, unloading region, and transitional region, as shown in Fig. 1 [2]. The transitional region connects the loading region with unloading region and deforms under the constraints of two adjacent regions. As a result, the material in transitional region undergoes complex material

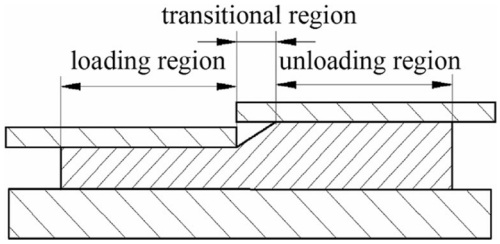

Fig. 1 Illustration of the local loading forming [2]

flow and large uneven deformation. The large and complex uneven deformation may produce some macro-defects such as folding. And more importantly, it may lead to non-uniform microstructure due to the strong microstructure sensitivity of titanium alloy to deformation amount. Therefore, the deformation inhomogeneity and forming quality of transitional region need more concern as it may determine the performance of component during local loading forming.

By now, lots of researches have been conducted on the deformation characteristics during integral forging process. For example, Zhang et al. [8] revealed the production mechanisms of folding and underfilling defects during the isothermal forging of aluminum alloy ring seat by FE simulation. Kim et al. [9] analyzed and predicted the defects during the multistep forging process of subminiature screws. The formation and avoidance of bulging and unfilled defects in the cold forging of an AUV blade pin head were studied by Abdullah et al. [10]. Chan et al. [11] investigated the effects of tooling geometry parameters on the formation of folding defect in the forging of axisymmetrical flanged components. Yang et al. [12] optimized the preform shapes by the combination of FE simulation and RSM to improve the deformation homogeneity in the forging of a typical aeroengine disk. On the other hand, some primary studies have been conducted on the forming characteristics of transitional region during local loading forming of large-scale rib-web components. Zhang et al. [13, 14] found that there exists transverse material flow in the transitional region due to the local loading characteristic, which is from the loaded region into the unloaded region. Gao et al. [15] further revealed the material flow mechanism of transitional region quantitatively by FE simulation combined with a user subroutine. Based on the material flow laws, the formation mechanisms of forming defects (folding and cavum) in transitional region are uncovered, and the influence of processing parameters on forming defects are studied through the combination of physical experiment and FE simulation [16]. In addition, Gao et al. [17] developed a quick prediction model for the folding defect of transitional region during local loading forming of large-scale rib-web component based on folding index. These works provide good guidance for predicting and avoiding the forming defects in transitional region. Nevertheless, the deformation inhomogeneity of transitional region during local loading forming has not been paid enough attention in the informed research studies. Sun et al. [18] investigated the influence of various processing parameters (forging mode, friction, and loading pass) on the final inhomogeneity of strain distribution on the whole bulk-head component after local loading forming by FE simulation. However, they do not consider the deformation inhomogeneity of transitional region, which is the most outstanding forming feature and closely related to the local loading characteristic. On the other side, the die parameters (fillet radius and draft angle) have great influence on the material flow and deformation behavior in the local loading forming of rib-web component [19]. It may be a feasible way to decrease the deformation inhomogeneity by adjusting the die parameters. Therefore, further investigation is required to reveal the mechanism of deformation inhomogeneity in transitional region, and its dependence rules on the die parameters during local loading forming of titanium alloy large-scale rib-web component.

In this paper, the deformation inhomogeneity of transitional region in the local loading forming of TA15 alloy large-scale rib-web component was studied by FE simulation. An area-weighted strain inhomogeneity index was applied to represent the deformation inhomogeneity, which is calculated based on user subroutine of DEFORM-2D. Then, the mechanism of deformation inhomogeneity in transitional region and its dependence rules on the die parameters were analyzed quantitatively. Besides, the relationship between the die parameters and deformation inhomogeneity is established, based on which the optimal die parameters for improving deformation homogeneity were determined. The results will provide basis for improving the homogeneities of deformation and microstructure in the isothermal local loading forming of titanium alloy large-scale rib-web component.

2 Research method

2.1 FE simulation of the transitional region

FE simulation has been widely applied to analyze the forming characteristics in metal forming, which can predict the distribution of strain and velocity, and the evolution of defects during forming process [20–22]. The FE model of transitional region in the local loading forming of large-scale rib-web component has been developed in previous studies, as shown in Fig. 2 [15–17]. It has been successfully applied to study the mechanisms of material flow and defects formation in transitional region [15, 16]. In the FE model, the lower die is integral, while the top die is divided into two symmetrical parts: Top die 1 and Top die 2. The local loading forming is conducted in one loading step including two loading steps. The local loading on workpiece is achieved by adjusting the relative position of two top dies using a spacer block, as shown in Fig. 2. The structural geometry dimensions of die are shown in Fig. 2a. The billet height (H) is 30 mm. Both of the reduction

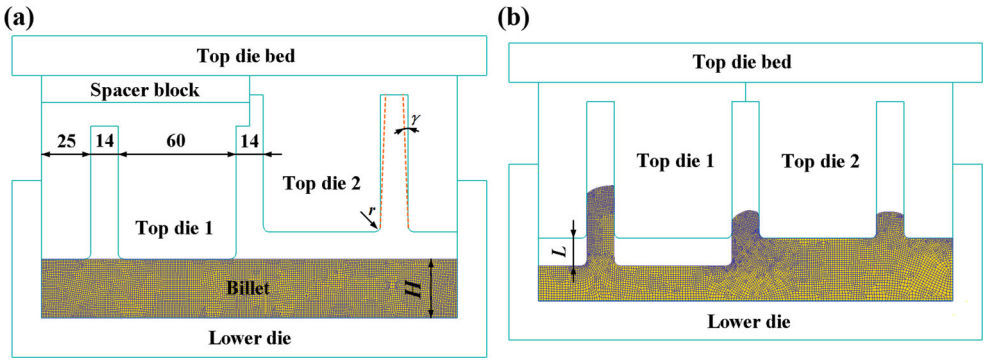

Fig. 2 2D FE model of transitional region in the local loading forming of large-scale rib-web component. **a** The first loading step. **b** The second loading step [15]

amount and spacer block thickness are 13 mm. In FE modeling, the billet is set as rigid-plastic type, whose material model (TA15 alloy) is input in the form of discrete points based on the work of Shen [23]. Since the metal flow perpendicular to die partition boundary is the main deformation, the deformation in transitional region is simplified as a plane strain problem. The whole forming process is modeled in isothermal condition neglecting any thermal events, as the isothermal local loading is performed under high temperature and low loading speed. The von Mises yielding criteria and constant shear friction model are employed. To avoid the meshing-induced singularity, the automatic remeshing and local refined meshing techniques are used. The developed FE model has been verified reliable to simulate the material flow and deformation behavior in transitional region by physical experiments in the author's works [15–17]. So, this FE model is applied to predict the deformation inhomogeneity of transitional region in this work. To study the effect of die parameters, the fillet radius (r) and draft angles (γ) of three ribs vary from 3 to 9 mm and 1 to 3°, respectively. As for the processing parameters, the deformation temperature, loading speed, and friction factor are set as 950 °C, 0.1 mm/s, and 0.5, respectively, for all samples.

2.2 Evaluation of the deformation inhomogeneity

In this work, the deformation inhomogeneity of transitional regions is evaluated in the whole workpiece and different local regions, as marked Regions A–C in Fig. 3. Two regional boundaries (red lines) are parallel to vertical axis and locate in the middle of two adjacent ribs. Regions A–C are divided according to their different deformation histories in the local loading forming. The material in Region A undergoes large deformation in first loading step but small deformation in second loading step. The material in Region B undergoes moderate deformation under the constraints of Regions A and C in both two loading steps. However, the material in Region C undergoes small deformation in first loading step but large deformation in second loading step. Different deformation histories may lead to different characteristics of deformation inhomogeneity, thus the deformation inhomogeneities of Regions A–C are all calculated and analyzed in this work. The deformation inhomogeneity of Regions A, B, and C and the whole workpiece are noted as φ_A, φ_B, φ_C, and φ_T, respectively.

In the informed researches, the deformation inhomogeneity of forging workpiece is usually evaluated by the following indexes [12, 24]:

$$\varphi_1 = \sum_{i=1}^{N} \left(\overline{\varepsilon}_i - \overline{\varepsilon}_{\text{ave}}\right)^2 \tag{1}$$

$$\varphi_2 = \frac{1}{N}\sum_{i=1}^{N} \left(\overline{\varepsilon}_i - \overline{\varepsilon}_{\text{ave}}\right)^2,\ \overline{\varepsilon}_{\text{ave}} = \sum_{i=1}^{N} \varepsilon_i/N \tag{2}$$

$$\varphi_3 = \overline{\varepsilon}_{\max} - \overline{\varepsilon}_{\min} \tag{3}$$

$$\varphi_4 = \sum_{i=1}^{N} v_i\left(\overline{\varepsilon}_i - \overline{\varepsilon}'_{\text{ave}}\right)^2 \Big/ \sum_{i=1}^{N} v_i,\ \overline{\varepsilon}'_{\text{ave}} = \sum_{i=1}^{N} v_i\overline{\varepsilon}_i \Big/ \sum_{i=1}^{N} v_i \tag{4}$$

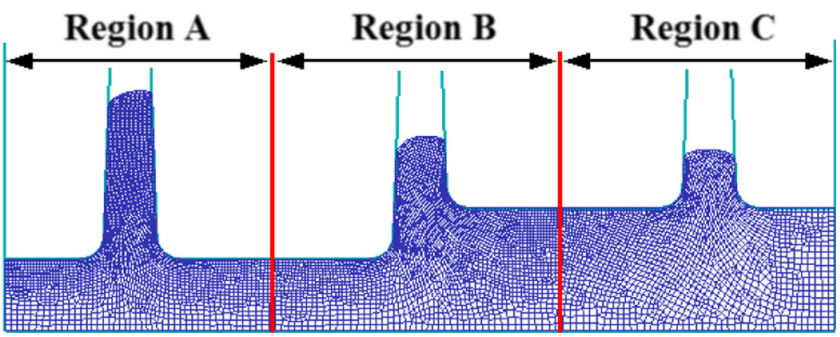

Fig. 3 Schematic of regional division in the workpiece

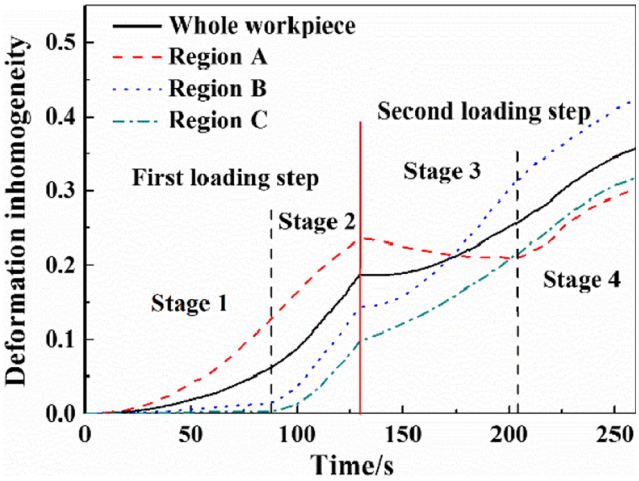

Fig. 4 The variation of deformation inhomogeneity during the local loading forming process

where $\bar{\varepsilon}_i$ and v_i are the effective strain and volume of element i, respectively, $\bar{\varepsilon}_{\max}$ and $\bar{\varepsilon}_{\min}$ are the maximum and minimum effective strain, respectively. The indexes of Eqs. (1)–(3) are all calculated based on the strain and number of elements. While, the volume of element is also considered in the index of Eq. (4). Here, the element volume is aiming at 3D FE simulation, which can be changed to element area in the 2D FE simulation. In this work, the element area may change with region and sample due to the uncertainty of element meshing in FE simulation. Moreover, there exist great differences on the number of elements and total area among different concerned regions. Therefore, the area-weighted inhomogeneity index Eq. (5) was applied to guarantee the comparability of inhomogeneity index among various regions and samples.

$$\varphi = \sum_{i=1}^{N} s_i \left(\bar{\varepsilon}_i - \bar{\varepsilon}''_{\text{ave}}\right)^2 / \sum_{i=1}^{N} s_i \tag{5}$$

where s_i is the area of element i, $\bar{\varepsilon}''_{\text{ave}}$ is the area-weighted average effective strain of all elements represented by $\bar{\varepsilon}''_{\text{ave}} = \sum_{i=1}^{N} s_i \bar{\varepsilon}_i / \sum_{i=1}^{N} s_i$.

The strain inhomogeneity indexes of different regions are calculated via user subroutine of DEFORM-2D in this work. In the subroutine, the effective strain of each element can be acquired directly from the subroutine, while the areas of each element and region are calculated by a previous proposed method by the authors [15]. The strain inhomogeneity indexes φ_A, φ_B, φ_C, and φ_T at each solution step are calculated and saved to analyze the evolution of deformation inhomogeneity.

3 Analysis of the deformation inhomogeneity in transitional region

In this section, the evolution and mechanisms of deformation inhomogeneity in transitional region are analyzed through a typical sample with the same fillet radius (r) of 6 mm and draft angle (γ) of 2° for three ribs. The billet height (H) and reduction amount are 30 and 13 mm, respectively.

Figure 4 shows the variations of deformation inhomogeneities of different regions during forming process. It can be found that they all increase gradually with the forming process but present time-changing and different rates. Based on the variation laws of deformation inhomogeneity and strain distribution during forming process, the whole local loading process can be broadly divided into four forming stages with two stages in each loading step, as shown in Fig. 4. The representative strain distribution of each forming stage is given in Fig. 5. For the first loading step, in stage 1, deformation mainly happens in Region A and its deformation inhomogeneity is also the largest. From Fig. 5a, it can be seen that the left rib

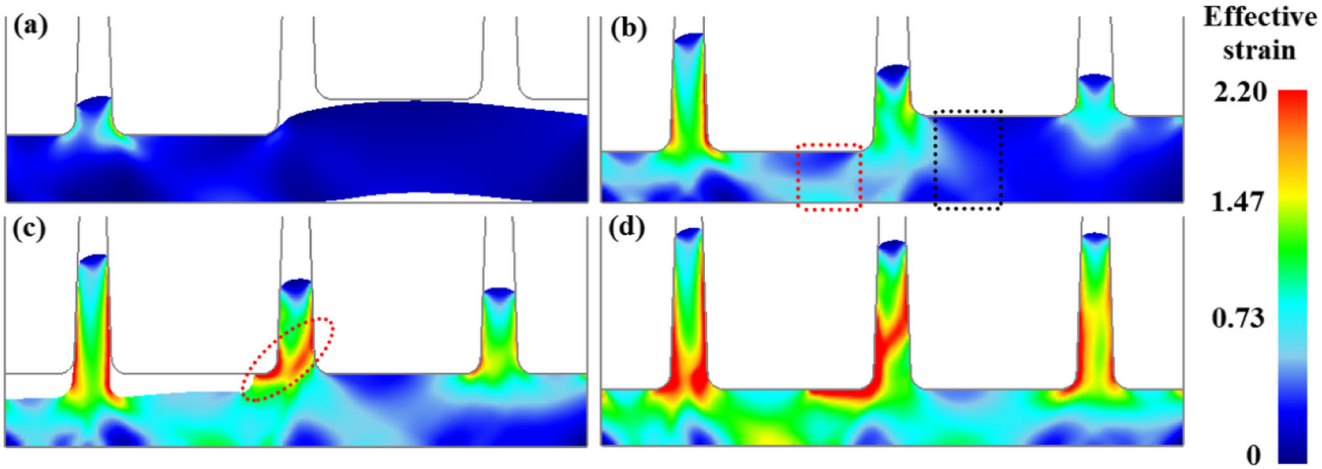

Fig. 5 The representative strain distribution at different forming stages: **a** stage 1, **b** stage 2, **c** stage 3, **d** stage 4

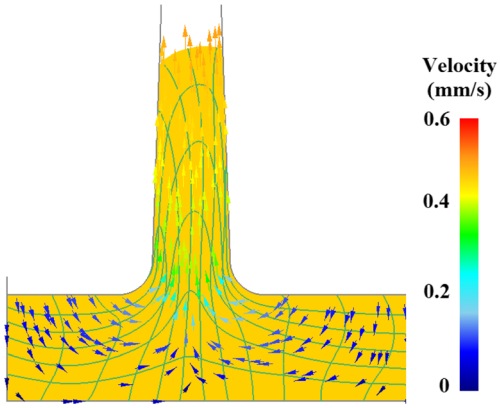

Fig. 6 The material flow pattern and grid change of Region A corresponding to Fig. 5b

was filled to some extent and a strain concentration area produces at its root in this stage, which is the main reason for the greater deformation inhomogeneity of Region A. With the increase of punch stroke, the material in Regions B and C also deforms to a lager extent (Fig. 5b), and their deformation inhomogeneities increase (Fig. 4). It can be seen from Fig. 5b that the strain distribution of Region C is similar to that of Region A with a strain concentration area at the root and sides of right rib. Nevertheless, the strain distribution of Region B is different to Regions A and C. In addition to the strain concentration area at the root of middle rib, the deformation amount under Top die 1 (red rectangle) is significantly greater than that under Top die 2 (black rectangle) due to the feature of local loading forming. This also contributes to the deformation inhomogeneity of Region B. At the end of first loading step, the order of deformation inhomogeneities at different regions is $\varphi_A > \varphi_T > \varphi_B > \varphi_C$, as shown in Fig. 4.

For the second loading step, in stage 3, Region A undergoes little deformation and its deformation inhomogeneity change little. While, large deformation happens in Regions B and C, and their deformation inhomogeneities increase gradually. It should be noted that the deformation inhomogeneity of Region B increases more quickly than that of Region C in this stage (Fig. 4). This is because a large-scale and significant strain concentration area generates at the middle rib (ellipse region in Fig. 5c), which does not exist in Region C. In the later forming stage, three regions deform simultaneously and their deformation inhomogeneities all increase further (Fig. 4). However, their strain distribution (Fig. 5d) is similar to those in stage 3 (Fig. 5c) and change little in this stage. At the end of local loading forming, the order of deformation inhomogeneities at different regions is $\varphi_B > \varphi_T > \varphi_C > \varphi_A$, as given in Fig. 4.

From the above analyses, it can be found that there exist two kinds of strain concentration area in the forming process, both of which play great roles in the deformation inhomogeneity. One kind is the strain concentration area at the root and sides of left and right ribs and another kind is the strain concentration area at the middle rib, as shown in Fig. 5d. To reveal their formation mechanisms, the material flow pattern and grid change of Region A and Region B are shown in Figs. 6 and 7, respectively. From Fig. 6, it can be seen that the material flow direction changes greatly at the fillet of rib root and the grid warps to some extent at this area. The horizontal grid lines get upwarp with the filling of rib; concurrently, the surface grids near the fillet were stretched severely. These suggest that large deformation happens in this region, which results in the strain concentration area at the root and sides of rib; moreover, the strain decreases from the outer surface to the interior of the rib, as shown in Fig. 5b.

As for the second kind of strain concentration area at the middle rib, it is closely related to the features of local loading forming. Figure 7a shows the material flow pattern and grid change of Region B in the first loading step. It can be found that the change of material flow direction and wrap of grids both occurs near the fillet of rib root, which is similar to the phenomenon in Region A (Fig. 6). However, due to the feature of local loading forming, the left fillet is lower than the right fillet in the first loading step. As a result, the wrap of grids and deformation amount at the web in Region B is asymmetric distribution, as mentioned above. In the second loading step (Fig. 7b), the web

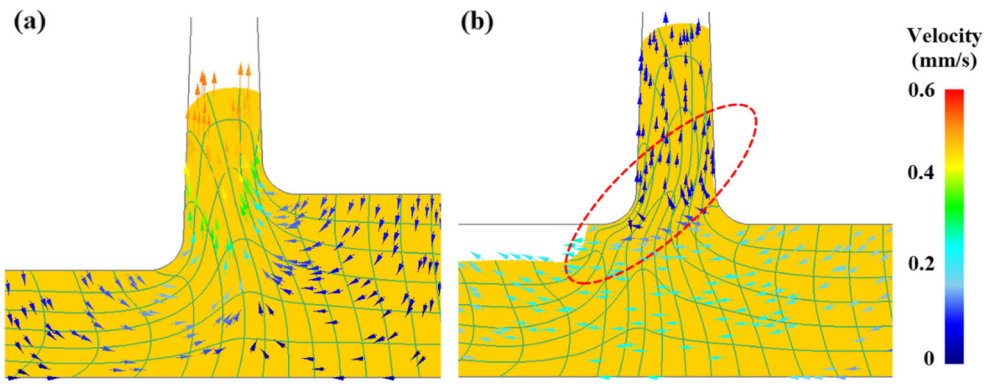

Fig. 7 The material flow pattern and grid change of Region B: **a** corresponding to Fig. 5b; **b** corresponding to Fig. 5c

Table 1 Factors and levels of orthogonal experiment

Factors	Level 1	Level 2	Level 3
Factor A			
Draft angle of left rib γ_1 (°)	1	2	3
Factor B			
Radius of left rib r_1 (mm)	3	6	9
Factor C			
Draft angle of middle rib γ_2 (°)	1	2	3
Factor D			
Radius of middle rib r_2 (mm)	3	6	9
Factor E			
Draft angle of right rib γ_3 (°)	1	2	3
Factor F			
Radius of right rib r_3 (mm)	3	6	9

material in Region B fill into the middle rib and move left at the same time due to the gap between top die 1 and the workpiece. Concomitantly, a step is formed between the left rib and middle rib. From Fig. 7b, it can be found that the grids near the step and rib root get slant wrap seriously (ellipse region). Thus, a slant strain concentration area was produced near the step and rib root in Region B, as shown in Fig. 5c.

4 Effects of die parameters on the deformation inhomogeneity

4.1 Orthogonal experiment design

The orthogonal experiment design can study the effect of many factors simultaneously in a single set of experiments with much fewer experiment units, which has been extensively used in various fields [25, 26]. In this study, the effect of fillet radius and draft angles of three ribs in transitional region is concerned. The $OA_{18}(3^7)$ matrix, which is an orthogonal array of seven factors and three levels, was employed to assign the considered factors and levels, as shown in Table 1. The detailed experiment scheme and calculated results of deformation inhomogeneity are given in Table 2. According to the calculated results, the effect law and significance of factors on the deformation inhomogeneity will be analyzed below.

4.2 Discussion

In the analysis of orthogonal experiment, the range analysis is usually applied to study the effect significance and law of factors on the target value [25, 26]. There are two important parameters in a range analysis, i.e., K_{ji} and R_j. K_{ji} is defined as the sum of the indexes of all levels (i, $i = 1, 2, 3$) in each factor j and K_{ji} is the average value of K_{ji} at the same level i. The

Table 2 Orthogonal experiment schemes and simulated results of deformation inhomogeneity

No.	Factors						Deformation inhomogeneity			
	γ_1 (°)	r_1 (mm)	γ_2 (°)	r_2 (mm)	γ_3 (°)	r_3 (mm)	φ_A	φ_B	φ_C	φ_T
1	1	3	1	3	1	3	0.34	0.42	0.31	0.36
2	1	6	2	6	2	6	0.33	0.40	0.31	0.35
3	1	9	3	9	3	9	0.33	0.41	0.34	0.37
4	2	3	1	6	2	9	0.32	0.43	0.31	0.37
5	2	6	2	9	3	3	0.31	0.41	0.33	0.36
6	2	9	3	3	1	6	0.29	0.38	0.31	0.33
7	3	3	2	3	3	6	0.31	0.48	0.35	0.40
8	3	6	3	6	1	9	0.30	0.39	0.32	0.34
9	3	9	1	9	2	3	0.32	0.39	0.31	0.35
10	1	3	3	9	2	6	0.37	0.38	0.33	0.37
11	1	6	1	3	3	9	0.30	0.44	0.34	0.38
12	1	9	2	6	1	3	0.30	0.39	0.31	0.34
13	2	3	2	9	1	9	0.32	0.35	0.30	0.33
14	2	6	3	3	2	3	0.30	0.40	0.33	0.35
15	2	9	1	6	3	6	0.30	0.45	0.32	0.37
16	3	3	3	6	3	3	0.33	0.47	0.38	0.40
17	3	6	1	9	1	6	0.31	0.37	0.30	0.34
18	3	9	2	3	2	9	0.31	0.44	0.32	0.37

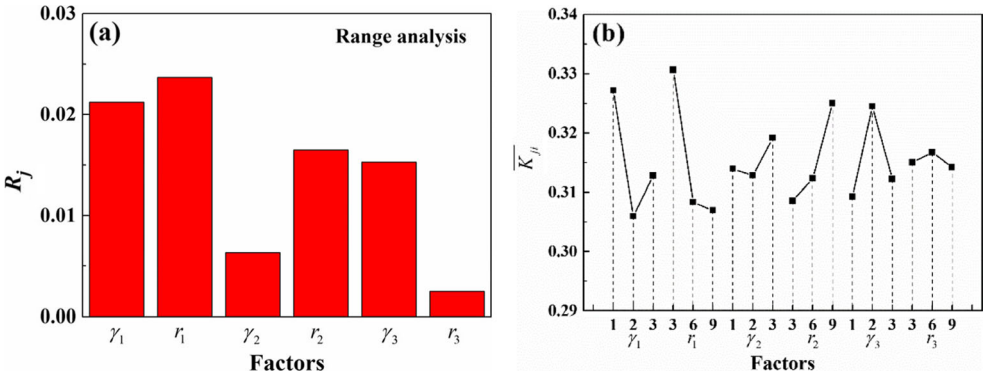

Fig. 8 Range analysis results on the deformation inhomogeneity of Region A: **a** range values of different factors; **b** the relationship between deformation inhomogeneity and levels of different factors

range value (R_j) is the range between the maximum and minimum value of K_{ji}. R_j can be used to evaluate the significance of factors, i.e., a larger R_j means a greater significance of the factor. Taking the $OA_{18}(3^7)$ matrix as an example, the calculations for factor A is as follows:

$$\begin{aligned} K_{A1} &= Y_1 + Y_2 + Y_3 + Y_{10} + Y_{11} + Y_{12} \\ K_{A2} &= Y_4 + Y_5 + Y_6 + Y_{13} + Y_{14} + Y_{15} \\ K_{A3} &= Y_7 + Y_8 + Y_9 + Y_{16} + Y_{17} + Y_{18} \\ K_{A1} &= K_{A1}/3;\quad K_{A2} = K_{A2}/3;\quad K_{A3} = K_{A3}/3 \\ R_j &= \max\left(K_{Ai}\right) - \min\left(K_{Ai}\right) \end{aligned} \tag{6}$$

where K_{Ai} is the K value of level i of factor A and Y_i is the result of trial No. i. K values of other factors can be determined by the same calculation steps.

Figure 8 shows the range analysis results on the deformation inhomogeneity of Region A. Comparing the range values of different factors (Fig. 8a), it can be found that r_1 and γ_1 are two most significant factors for φ_A. From Fig. 8b, it can be found that φ_A decreases with the increases of r_1. As mentioned above, the deformation inhomogeneity of Region A is mainly produced by the strain concentration area at the root and sides of rib. The increase of r_1 is beneficial to the filling of rib and can reduce the grid distortion degree at the root and sides of rib. This would relieve the strain concentration at the root and sides of rib and then decrease the deformation inhomogeneity.

As for the influence of γ_1, φ_A first decreases and then increases with the increase of γ_1, as shown in Fig. 8b. This is because γ_1 have two competitive influence mechanisms on the strain concentration at Region A. One side, increasing γ_1 can reduce the direction change degrees of material flow and grid distortion at the rib root, which is helpful to relieving the strain concentration and deformation inhomogeneity. On the other hand, greater γ_1 would increase the flow resistance of surface material of rib and increases the grid distortion degree at the sides of the rib. This would increase the strain concentration and deformation inhomogeneity. At smaller γ_1, the first mechanism plays a greater role, so φ_A decreases with the increases of γ_1 first. With the increase of γ_1, the role of second mechanism increases gradually and becomes the leading role, thus φ_A increases with γ_1 at greater γ_1.

The results of range analysis on the deformation inhomogeneity of Region B (φ_B) are given in Fig. 9. It can be seen from Fig. 9a that the most significant factor for φ_B is γ_3. According to the variation of φ_B during the local loading forming (Fig. 4), we can find that the deformation in the second loading step plays a leading role in the final φ_B. As demonstrated in Section 3, there exists a leftward transverse material flow at the web in the second loading step. This would produce a slant strain concentration area near the step and rib root in Region B, thus resulting in the increase of φ_B. The increase of γ_3 would suppress the filling of the right rib and increase the amount of leftward material flow, which would

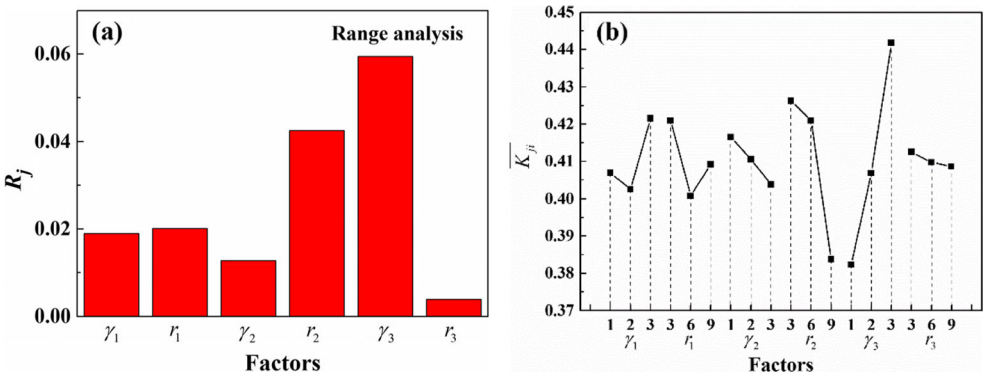

Fig. 9 Range analysis results on the deformation inhomogeneity of Region B: **a** range values of different factors; **b** the relationship between deformation inhomogeneity and levels of different factors

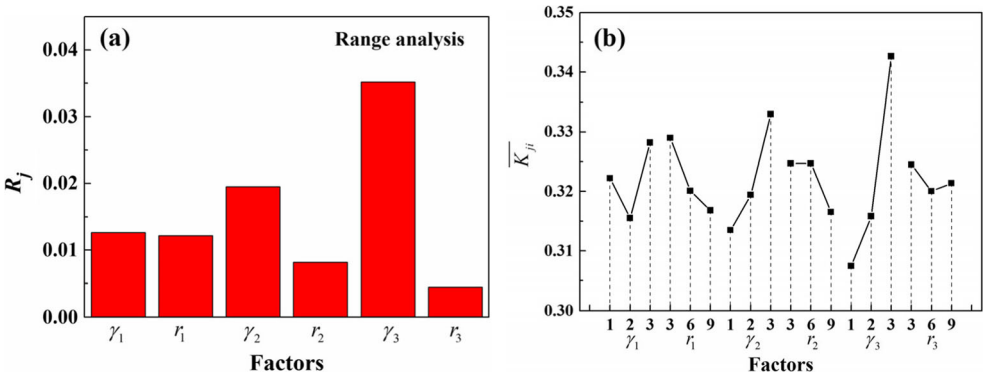

Fig. 10 Range analysis results on the deformation inhomogeneity of Region C: **a** range values of different factors; **b** the relationship between deformation inhomogeneity and levels of different factors

intensify the strain concentration and increase φ_B. Therefore, φ_B increases with the increase of γ_3, as given in Fig. 9b. Besides, we can also find that r_2 presents a greater impact on φ_B, i.e., φ_B decreases with the increase of r_2. This is similar to the influence law of r_1 on φ_A. The increases of r_2 could relieve the strain concentration at the root and sides of middle rib and then decreases φ_B.

Figure 10 shows the range analysis results on the deformation inhomogeneity of Region C (φ_C). The range values in Fig. 10a indicate that γ_3 is the most significant factor for φ_C. As demonstrated in Section 3, the strain concentration feature of Region C is close to that of Region A due to their similar deformation behavior. Thus, γ_3 should also present the competitive influence mechanisms on the strain concentration at Region C as that of γ_1 for Region A. It can be seen from Fig. 10b that φ_C increases with γ_3 monotonously. This suggests that the second mechanism, i.e., the greater draft angle increases the grid distortion and strain concentration degree at the sides of rib, plays the decisive role in φ_C.

Figure 11 gives the range analysis results on the deformation inhomogeneity of the whole workpiece (φ_T). According to the range values in Fig. 11a, it can be concluded that γ_3 is the most significant factor for φ_T, which is the same to φ_B and φ_C. Moreover, the influence law of γ_3 on φ_T is also the same to those of φ_B and φ_C, i.e., φ_T increases with γ_3. In addition to γ_3, the factors γ_1, r_1, and r_2 also influence φ_T to some extent but does not present monotonous changing law.

Based on the above analyses, it can be concluded that the die parameters play great roles in the deformation inhomogeneity of transitional region in the local loading forming of rib-web component. The significant influence factors for different local regions and the whole transitional region are different. Decreasing the draft angle of the right rib could improve the deformation homogeneity of the whole transitional region.

5 Optimization of die parameters to improve deformation homogeneity

At present, metamodeling techniques have been widely used to model the computation-intensive FE simulation with simple analytical models in order to improve efficiency. The metamodel can facilitate the design space exploration, process optimization and reliability analysis to a very great extent. RSM is one of the most popular metamodeling techniques for approximating the time-consuming FE simulation and the subsequent parameters optimization [12, 17, 27]. Thus, the optimization of die parameters based on RSM is applied to improve the deformation homogeneity of transitional region in this section.

The deformation inhomogeneity of transitional region (φ_T) is correlated with die parameters using RSM based on the

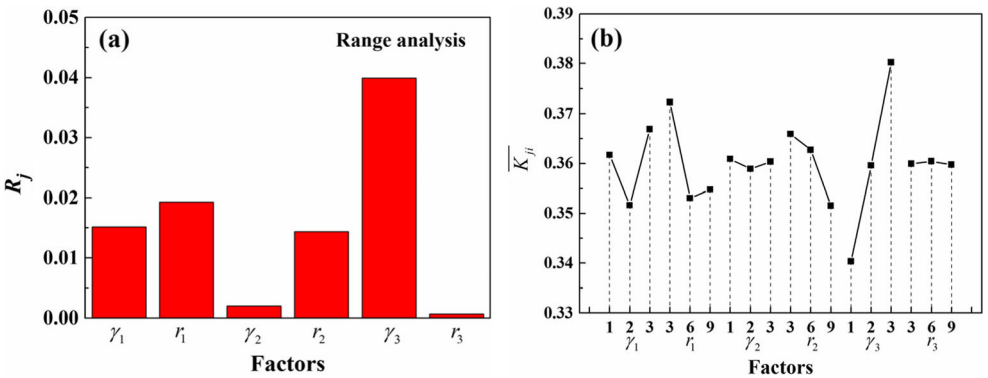

Fig. 11 Range analysis results on the deformation inhomogeneity of the whole workpiece: **a** range values of different factors; **b** the relationship between deformation inhomogeneity and levels of different factors

Table 3 ANOVA analysis for the RSM model

Source	Sum of squares	*df*	Mean square	*F* value	*p* value
Model	7.62×10^{-3}	10	7.62×10^{-4}	69	<0.0001
Residual	7.73×10^{-5}	7	1.10×10^{-5}		
Cor total	7.70×10^{-3}	17			

$R^2 = 0.9900$; adjusted $R^2 = 0.9756$

simulation results in Table 2. In the RSM modeling, the polynomial function is usually used as the approximate model for its simplicity. In this work, the quadratic polynomial is used with the following formulation:

$$y = \beta_0 + \sum_{j=1}^{k} \beta_j x_j + \sum_{j=1}^{k} \beta_{jj} {x_j}^2 + \sum_{i=1}^{k-1} \sum_{j=i+1}^{k} \beta_{ij} x_i x_j \tag{7}$$

where y is the response (φ_T), k is the number of input variables, x_i and x_j are the set of model input variables (γ_1, r_1, γ_2, r_2, γ_3, r_3), and β_0, β_j, β_{jj}, β_{ij} represent the regression coefficients. The stepwise regression method was employed here to get the final polynomial regression model:

$$\begin{aligned}\varphi_T = {} & 0.456 - 0.060 \times \gamma_1 - 0.017 \times r_1 - 0.020 \times \gamma_2 - 0.002 \times r_2 + 0.023 \times \gamma_3 - 0.004 \times r_3 \\ & + 0.013 \times \gamma_1^2 + 0.001 \times r_1^2 + 0.005 \times \gamma_2^2 + 0.002 \times \gamma_1 r_3\end{aligned} \tag{8}$$

The ANOVA analysis for response model is shown in Table 3. It can be found that the response model is significant as the p value is less than 0.01. The adequacy measures of R^2 and adjusted R^2 are in reasonable agreement and are both close to 1. These suggest that the model is adequate and meaningful.

To validate the developed RSM model, six additional random samples were designed within the whole design space (Section 2.1) by the general Latin Hypercube design through MATLAB software. Table 4 gives the schemes of random samples and the corresponding simulated values by FEM, predicted values by RSM, and the percentage error of RSM model. It can be observed that the predicted errors are very small between the simulated and predicted values with the average error of 3.85 %. It suggests that the developed RSM model is reliable to predict the deformation inhomogeneity of transitional region.

Then, the constrained optimization of deformation homogeneity of transitional region is defined as follows:

$$\left.\begin{array}{ll} \text{Variables} & \gamma_1, r_1, \gamma_2, r_2, \gamma_3, r_3 \\ \text{Min} & \varphi_T(\gamma_1, r_1, \gamma_2, r_2, \gamma_3, r_3) \\ \text{s.t.} & 1 \le \gamma_1, \gamma_2, \gamma_3 \le 3 \\ & 3 \le r_1,\ r_2, r_3 \le 9 \end{array}\right\} \tag{9}$$

The pattern search method in the optimization toolbox of MATLAB software is applied to solve the above optimization problem. The global optimum solutions are $\gamma_1 = 1.64°$, $r_1 = 7.22$ mm, $\gamma_2 = 2.04°$, $r_2 = 9$ mm, $\gamma_3 = 1°$, $r_3 = 9$ mm, and the minimum φ_T is 0.31. In order to verify the optimization result, FE simulation with the optimized die parameters was conducted. The corresponding simulated φ_T is 0.32, which is very close to the predicted value by RSM (0.31) with the error of 3.15 %. This indicates that the optimization result for the deformation homogeneity of transitional region in local loading forming is valid.

In the isothermal local loading forming of titanium alloy rib-web component, the transitional region undergoes complex and large inhomogeneous deformation, which may lead to some macro-defects such as folding. Moreover, it may lead to non-uniform microstructure due to the strong microstructure sensitivity of titanium alloy to deformation amount. On the other hand, the die parameters have great influence on the deformation behavior in the local loading forming. Thus, optimizing the die parameters to decrease the deformation inhomogeneity is of great significance to control the macro-defects and microstructure. However, this work is only focused on the influence of die parameters on the deformation inhomogeneity. Further works

Table 4 Comparisons of the prediction results obtained by RSM and FE simulation

No.	γ_1 (°)	r_1 (mm)	γ_2 (°)	r_2 (mm)	γ_3 (°)	r_3 (mm)	φ_T (FEM)	φ_T (RSM)	Error (%)
1	2.60	6.96	1.56	5.69	1.24	4.75	0.32	0.35	8.20
2	1.30	5.49	2.25	7.32	2.92	5.26	0.36	0.38	3.84
3	1.38	3.80	2.58	6.95	2.09	8.51	0.35	0.36	2.07
4	1.97	7.14	1.80	8.03	1.56	6.70	0.32	0.33	4.43
5	2.21	8.42	1.22	3.44	2.55	3.89	0.35	0.37	4.35
6	2.70	4.92	2.72	4.38	1.72	7.96	0.35	0.35	0.19
Average error									3.85

should be conducted to correlate the deformation inhomogeneity with the macro-defects and microstructure, which is helpful to improve the macro and micro forming quality during the isothermal local loading forming of titanium alloy components.

6 Conclusions

In this paper, the formation of deformation inhomogeneity of transitional region and its dependence on the die parameters in the local loading forming of Ti-alloy rib-web component were systematically investigated. The following conclusions can be drawn:

(1). The area-weighted strain inhomogeneity index is applicable to evaluate the deformation inhomogeneity of transitional region at different die parameters. The user subroutine based on FE software (DEFORM-2D) is developed to calculate the strain inhomogeneity index.

(2). The deformation inhomogeneity of transitional region is mainly caused by two kinds of strain concentration areas. One kind is the almost symmetric strain concentration area at the non-partitioned ribs, which can be essentially ascribed to the filling of rib. Another kind is the slant strain concentration area at the partitioned rib, which is related to the multi-step local loading in the forming process.

(3). The draft angle of the right rib is the most significant factor for both the deformation inhomogeneities of the whole transitional region and partitioned rib region. Moreover, these two deformation inhomogeneities both decrease with the decrease of draft angle of the right rib.

(4). The deformation inhomogeneity of transitional region was correlated with the die parameters using the response surface method. Based on the developed RSM model, the optimal die parameters for improving deformation homogeneity of transitional region are determined as $\gamma_1 = 1.64°$, $r_1 = 7.22$ mm, $\gamma_2 = 2.04°$, $r_2 = 9$ mm, $\gamma_3 = 1°$, $r_3 = 9$ mm.

Acknowledgments The authors would like to gratefully acknowledge the support of National Natural Science Foundation of China (No. 51605388, 51575449), 111 Project (B08040), Project supported by the Research Fund of the State Key Laboratory of Solidification Processing (NWPU), China (Grant No. 131-QP-2015), the Fundamental Research Funds for the Central Universities, and the Open Research Fund of State Key Laboratory of Materials Processing and Die & Mould Technology, Huazhong University of Science and Technology.

Reference

1. Yang H, Fan XG, Sun ZC, Guo LG, Zhan M (2011) Recent developments in plastic forming technology of titanium alloys. Sci China-Technol Sci 54:490–501
2. Sun ZC, Yang H (2009) Microstructure and mechanical properties of TA15 titanium alloy under multi-step local loading forming. Mater Sci Eng A 523:184–192
3. Zhang DW, Yang H, Sun ZC (2010) Analysis of local loading forming for titanium-alloy T-shaped components using slab method. J Mater Process Technol 210:258–266
4. Zhang DW, Yang H, Sun ZC, Fan XG (2012) Deformation behavior of variable-thickness region of billet in rib-web component isothermal local loading process. Int J Adv Manuf Technol 63(1–4):1–12
5. Zhang DW, Yang H (2013) Metal flow characteristics of local loading forming process for rib-web component with unequal-thickness billet. Int J Adv Manuf Technol 68(9–12):1949–1965
6. Zhang DW, Yang H (2013) Numerical study of the friction effects on the metal flow under local loading way. Int J Adv Manuf Technol 68:1339–1350
7. Fan XG, Yang H, Sun ZC, Zhang DW (2010) Effect of deformation inhomogeneity on the microstructure and mechanical properties of large-scale rib-web component of titanium alloy under local loading forming. Mater Sci Eng A 527:5391–5399
8. Zhang YQ, Jiang SY, Zhao YA, Shan DB (2014) Isothermal precision forging of aluminum alloy ring seats with different preforms using FEM and experimental investigation. Int J Adv Manuf Technol 72:1693–1703
9. Kim JB, Seo WS, Park K (2012) Damage prediction in the multi-step forging process of subminiature screws. Int J Precis Eng Manuf 13(9):1619–1624
10. Abdullah AB, Sapuan SM, Samad Z, Khaleed HMT, Aziz NA (2013) Numerical investigation of geometrical defect in cold forging of an AUV blade pin head. J Manuf Process 15(1):141–150
11. Chan WL, MW F, Lu J, Chan LC (2009) Simulation-enabled study of folding defect formation and avoidance in axisymmetrical flanged components. J Mater Process Technol 209(11):5077–5086
12. Yang YH, Liu D, He ZY, Luo ZJ (2010) Optimization of preform shapes by RSM and FEM to improve deformation homogeneity in aerospace forgings. Chinese J Aeronaut 23:260–267
13. Zhang DW, Yang H, Sun ZC, Fan XG (2011) Deformation behavior under die partitioning boundary during titanium alloy large-scale rib-web component forming by isothermal local loading. Proceedings of the 12th World Conference on Titanium. Beijing: Science Press, pp. 328
14. Zhang DW, Yang H (2014) Distribution of metal flowing into unloaded area in the local loading process of titanium alloy rib-web component. Rare Metal Mater Eng 43(2):296–300
15. Gao PF, Yang H, Fan XG (2014) Quantitative analysis of the material flow in transitional region during isothermal local loading forming of Ti-alloy rib-web component. Int J Adv Manuf Technol 75(9–12):1339–1347
16. Gao PF, Yang H, Fan XG, Lei PH (2014) Forming defects control in transitional region during isothermal local loading of Ti-alloy rib-web component. Int J Adv Manuf Technol 76(5–8):857–868
17. Gao PF, Yang H, Fan XG, Lei PH (2015) Quick prediction of the folding defect in transitional region during isothermal local loading forming of titanium alloy large-scale rib-web component based on folding index. J Mater Process Technol 219:101–111
18. Sun ZC, Yang H, Sun NG (2012) Effects of parameters on inhomogeneous deformation and damage in isothermal local loading forming of Ti-Alloy component. J Mater Eng Perform 21:313–323
19. Zhang DW, Yang H, Sun ZC, Fan XG (2011) Influences of fillet radius and draft angle on local loading process of titanium alloy T-shaped components. Trans Nonferrous Met Soc China 21:2693–2704
20. Saxena RK, Dixit PM (2009) Finite element simulation of earing defect in deep drawing. Int J Adv Manuf Technol 45:219–233

21. Zhou J, Wang F, Wang M, Xu W (2011) Study on forming defects in the rolling process of large aluminum alloy ring via adaptive controlled simulation. Int J Adv Manuf Technol 55:95–106
22. Li F, Lin JF, Yuan SJ, Liu XJ (2009) Effect of inner cone punch on metal flow in extrusion process. Int J Adv Manuf Technol 42:489–496
23. Shen, CW (2007) Research on material constitution models of TA15 and TC11 titanium alloys in hot deformation process. Master Thesis, Northwestern Polytechnical University
24. Yang YH, Liu D, He ZY, Luo ZJ (2011) Evaluation of microstructure homogeneity in TC11 titanium alloy blisk forging. J Aeronaut Mater 32: 25–29 (in Chinese)
25. Wu X, Leung D (2011) Optimization of biodiesel production from camelina oil using orthogonal experiment. Appl Energ 88:3615–3624
26. Shen Q, Zheng Y, Li S, Ding H, Xu Y, Zheng C, Thern M (2016) Optimize process parameters of microwave-assisted EDTA method using orthogonal experiment for novel BaCoO3-δ perovskite. J Alloy Comp 658:125–131
27. Wang H, Li GY, Zhong ZH (2008) Optimization of sheet metal forming processes by adaptive response surface based on intelligent sampling method. J Mater Process Technol 197:77–88